Dynamics in the melt of an icosahedral $Al_{72}Pd_{20}Mn_8$ quasicrystal

2006 J. Phys.: Condens. Matter 18 L613

(http://iopscience.iop.org/0953-8984/18/49/L03)

INSTITUTE OF PHYSICS PUBLISHING JOURNAL OF PHYSICS: CONDENSED MATTER

J. Phys.: Condens. Matter **18** (2006) L613–L618 doi:10.1088/0953-8984/18/49/L03

LETTER TO THE EDITOR

Dynamics in the melt of an icosahedral $Al_{72}Pd_{20}Mn_8$ quasicrystal

J T Okada[1,6], M Inui[2], D Ishikawa[1], A Q R Baron[1,3], K Matsuda[4], S Tsutsui[3], Y Watanabe[5], S Nanao[5] and T Ishikawa[1,3]

[1] RIKEN/SPring-8, 1-1-1, Kouto, Mikazuki, Sayo, Hyogo 679-5198, Japan
[2] Graduate School of Integrated Arts and Sciences, Hiroshima University, 1-7-1, Kagamiyama, Higashi-Hiroshima 739-8521, Japan
[3] SPring-8/JASRI, 1-1-1, Kouto, Sayo-cho, Sayo-gun, Hyogo 679-5198, Japan
[4] Graduate School of Engineering, Kyoto University, Yoshida, Sakyo-ku, Kyoto 606-8501, Japan
[5] Institute of Industrial Science, The University of Tokyo, 4-6-1, Komaba, Meguro-ku, Tokyo 153-8505, Japan

E-mail: jt.okada@phys.mm.t.u-tokyo.ac.jp

Received 10 September 2006, in final form 9 November 2006
Published 23 November 2006
Online at stacks.iop.org/JPhysCM/18/L613

Abstract

The dynamic structure factor $S(Q, \omega)$ of the melt of an icosahedral quasicrystal, $Al_{72}Pd_{20}Mn_8$, was measured at 1223 K near the melting point, $T_m = 1140$ K, for momentum transfers, Q, from 1.5 to 27.15 nm^{-1} by means of an inelastic x-ray scattering technique using synchrotron radiation at SPring-8. The composition of $Al_{72}Pd_{20}Mn_8$ is a special one in AlPdMn ternary alloys, since an icosahedral AlPdMn quasicrystal is formed from the melt. The acoustic mode was observed in the low-Q region, and a substantial broadening of the longitudinal current–current correlation function and the crossover of the effective sound velocity from hydrodynamic to viscoelastic regions were observed around 6 nm^{-1}, which hints at the existence of a cluster with a size of about 1 nm in the melt.

Quasiperiodic structures with icosahedral symmetry incompatible with the extended periodicity of the crystal were discovered by Shechtman *et al* in 1984 [1]. The frame structures of icosahedral quasicrystals (QCs) are built with icosahedral clusters that are several nanometres in diameter [2]. Prior to the discovery of QCs, it was believed that only crystals are the stable solid form in thermal equilibrium. At present, however, it is widely known that QCs exist as an equilibrium phase [2], and stable icosahedral QCs can be made from melts. $Al_{72}Pd_{20}Mn_8$ QC is known as a typical one being made from the melt; a large single icosahedral QC can be made in the composition of $Al_{72}Pd_{20}Mn_8$ [3]. Quite recently, the viscosity of a melt of icosahedral $Al_{72}Pd_{20}Mn_8$ QC was measured [4]. The viscosity increases substantially with

[6] Address for correspondence: Department of Advanced Material Sciences, The University of Tokyo, 5-1-5 Kashiwanoha, Chiba 277-8651, Japan.

decreasing temperature. It becomes about 2.5 cP at 1373 K, which is above the melting point of 1140 K; this is one order larger in magnitude than that of liquid aluminium near the melting point of 993 K [5]. Such high viscosity hints that cluster-like medium-range order exists in the $Al_{72}Pd_{20}Mn_8$ melt. Our interest is now directed to the process of how QCs are formed from the melt and the question if specific embryos, such as icosahedral clusters, exist in the melts.

To solve such a fundamental problem investigations of microscopic structures in several QC melts have been made by several researchers using neutron and x-ray diffraction techniques [6–9]. From the detailed analysis of the structure factor of QC melts the authors have claimed that icosahedral short-range order could exist in the melt. In addition to the information on the static structures, that on the dynamical structure is important and helpful in understanding the process of QC formation from the melts. To clarify the melt dynamics, we have performed inelastic x-ray scattering (IXS) experiments for the melt of icosahedral $Al_{72}Pd_{20}Mn_8$ QC. We have obtained the dynamical structure factor $S(Q, \omega)$ for the first time. In this letter, we report the results of $S(Q, \omega)$ for the $Al_{72}Pd_{20}Mn_8$ melt and discuss the existence of clusters in the melt.

The present work has been done at the high-resolution IXS beam line (BL35XU) of SPring-8 in Japan [10]. Back-scattering at the Si(11 11 11) reflection was used to provide a beam of 3×10^9 photons s^{-1} in a 0.8 meV bandwidth onto the sample. The energy of the incident beam and the Bragg angle of the backscattering were 21.747 keV and 89.98°, respectively. We used four spherical analyser crystals at the end of the 10 m horizontal arm to analyse the scattered x-rays. The spectrometer resolution depended on the analyser crystals, and it was 1.5–1.7 meV, which was obtained from a measurement on polymethyl methacrylate. The momentum resolution was set at 0.6 nm^{-1} in the Q region lower than 5.5 nm^{-1} and at 1.1 nm^{-1} in the higher region using slits.

A stainless chamber designed for IXS measurements at BL35XU was used to hold the sample and the heater in the oxygen-free atmosphere. An $Al_{72}Pd_{20}Mn_8$ sample of 330 μm in thickness was mounted in a single-crystal sapphire cell [11] and He gas at 1 atm and with 99.9999% purity was used for suppressing the evaporation of the sample. It was checked that the $Al_{72}Pd_{20}Mn_8$ melt does not react with sapphire by using differential thermal analysis. The cell was inserted into a Mo tube to keep the temperature uniform in the cell, and the tube was heated with Kanthal wire. The temperature of the sample was measured with two thermocouples attached to the top and bottom of the sapphire cell. The sample was maintained at 1340 K for 1 h to make the melt stable in the thermal equilibrium before starting the measurements at 1223 K.

Selected IXS data are shown in figure 1(a). The integral, $S(Q)$, of the spectrum, $S(Q, \omega)$, was used for the normalization, and $S(Q, \omega)/S(Q)$ values are plotted by open circles in a logarithmic scale. The resolution function obtained from a measurement of polymethyl methacrylate is shown by dots. The elastic peaks of the spectra are sharp and the line width of the spectra is nearly the same as that of the resolution function in the low-Q region. It is noted that weak shoulders representing an acoustic mode appear in the low-Q region. The data analysis was performed following the memory function approach [12, 13]. The spectrum $S(Q, \omega)$ can be expressed using the real and imaginary parts of $\tilde{M}(Q, \omega)$, the Fourier transform of the full memory function $M(Q, t)$. We took

$$\frac{S(Q,\omega)}{S(Q)} = \frac{\pi^{-1}\omega_0^2 \tilde{M}'(Q,\omega)}{[\omega^2 - \omega_0^2 + \omega\tilde{M}''(Q,\omega)]^2 + [\omega\tilde{M}'(Q,\omega)]^2}, \tag{2}$$

where $\tilde{M}'(Q, \omega)$ and $\tilde{M}''(Q, \omega)$ are the real and imaginary parts of $\tilde{M}(Q, \omega)$, and $\omega_0^2(Q) = \frac{k_B T Q^2}{m S(Q)}$, where m is the atomic mass. We have allowed a relaxation mechanism of non-thermal

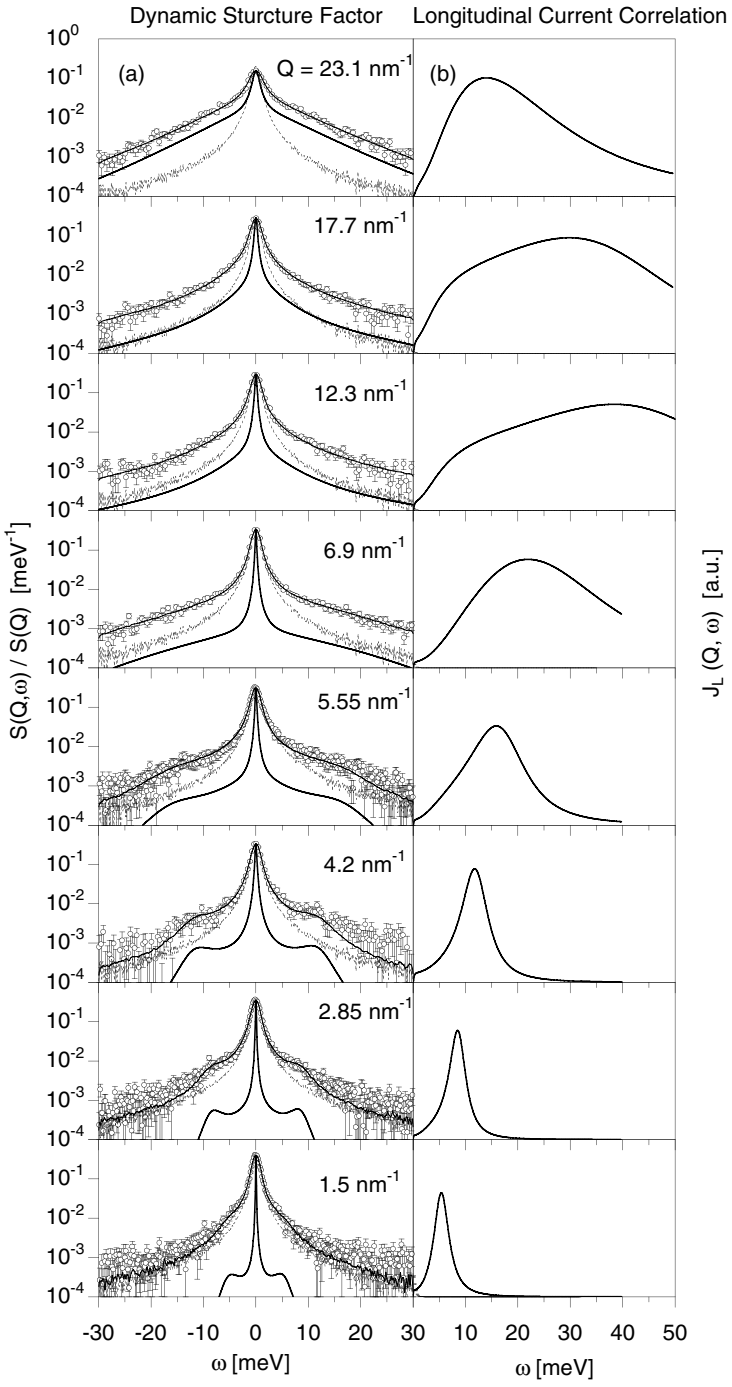

Figure 1. (a) IXS spectra (open circles) of the melt of an icosahedral $Al_{72}Pd_{20}Mn_8$ QC at 1223 K after background subtraction. The experimental data are normalized to their integrated intensity. Fits (solid lines) were made by convoluting the resolution function (dots) to a model function (thick solid lines) as discussed in the text. (b) The longitudinal current–current correlation function, J_l, (Q, ω), at different Q.

contributions by assuming that

$$M(Q,t) = (\gamma - 1)\omega_0^2(Q)\mathrm{e}^{-D_T Q^2} + \Delta^2(Q)A(Q)\mathrm{e}^{-t/\tau_\alpha(Q)}. \tag{3}$$

where γ, D_T, Δ^2, A and τ_α are the specific-heat ratio, the thermal conductivity, the total viscous strength, the relative weight of the viscous processes, and the relaxation times, respectively. By fitting this model function expressed by (2) to the experimentally obtained spectrum, we can deduce an optimized model function $S(Q,\omega)$ giving a resolution-free dynamic structure factor. In figure 1(a), thick solid lines indicate the model functions and solid lines show those obtained by convoluting the resolution function to the model function. As seen in figure 1(a), each experimental spectrum is well reproduced by using the corresponding model function. In the fitting, the χ^2 per degrees of freedom took values that are in between 1.0 and 1.4 for different Q. The parameters were deduced through the fitting procedure. The value of τ_α changed from 3 to 0.6 ps with increasing Q.

The model function was used to determine the longitudinal current–current correlation function, $J_l(Q,\omega)$, expressed by

$$J_l(Q,\omega) = \frac{\omega^2}{Q^2}S(Q,\omega). \tag{4}$$

The maximum of $J_l(Q,\omega)$ is considered to give a characteristic frequency ω_p relating to the effective sound velocity, $v(Q) = \omega_p(Q)/Q$. Figure 1(b) shows $J_l(Q,\omega)$ with different Q, each of which is obtained from the corresponding model function in figure 1(a). In the figure we can see characteristic features in the variation of $J_l(Q,\omega)$ with increasing Q. In the low-Q region ($Q = 1.5$, 2.85 and 4.2 nm^{-1}) the width of $J_l(Q,\omega)$ is narrow. The maximum is clearly seen and the peak position shifts to the large-ω side with increasing Q. In the larger-Q region ($Q = 5.55$ and 6.9 nm^{-1}) the shape is substantially changed. It becomes broad but the single maximum is still clearly seen and the peak position shifts to the large-ω side with increasing Q. At $Q = 12.3$ and 17.7 nm^{-1} the shape becomes quite broad. At $Q = 23.1$ nm^{-1} it becomes narrow again and the maximum position shifts to the small-ω side.

To examine the variation of the $J_l(Q,\omega)$ profile more quantitatively we plot such quantities as the peak position, ω_p, and the full-width at half-maximum (FWHM) as a function of Q. Figure 2(a) shows the plots of ω_p versus Q. The error bar of ω_p at each Q was estimated from the admissible width of every fitting parameter when the value of χ^2 became as small as about 1. Figure 2(b) shows the plots of FWHM, in which plots in the Q range from 10 to 20 nm^{-1} are not presented because the shapes of the corresponding $J_l(Q,\omega)$ are not simple and are too broad to reasonably estimate the width. Figure 2(c) shows the effective velocity $v(Q)$. Figure 2(d) shows the $S(Q)$ of the $Al_{72.1}Pd_{20.7}Mn_{7.2}$ melt near the melting point [6]; the composition of this sample is almost the same as that of the present specimen.

As is seen in figure 2(a), ω_p increases linearly with increasing Q in the small-Q region and has a maximum at approximately $Q = 14$ nm^{-1}, which is located at half of the first peak position of $S(Q)$ in figure 2(d). Then, ω_p decreases and has a minimum around the peak position of $S(Q)$. Such correlation between Q-variations of ω_p and $S(Q)$ is often observed in liquid metals. As already seen in figure 1(b), the most remarkable feature is that the shape of $J_l(Q,\omega)$ becomes substantially broad with increasing Q in the small-Q region. It is evident from the plots of FWHM in figure 2(b) that such broadening occurs approximately at $Q = 6$ nm^{-1}, around which the FWHM dramatically increases. It is useful to see again plots of ω_p in figure 2(a) in the small-Q region around 6 nm^{-1}. We find that four points at Q lower than 6 nm^{-1} fall on a straight line and the next three points located at $Q = 6.9$, 8.2 and 9.5 nm^{-1} seem to positively deviate from this line, although the error bars of the three points are large compared with those of the former. These changes in ω_p and FWHM around

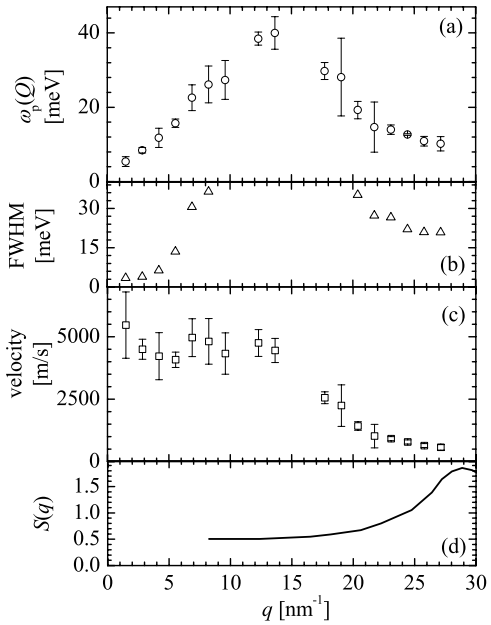

Figure 2. (a) The Q-dependence of ω_p for the melt of an icosahedral $Al_{72}Pd_{20}Mn_8$ QC at 1223 K. (b) Plots of FWHM of $J_l(Q, \omega)$. (c) The effective velocity, $v(Q) = \omega_p(Q)/Q$. (d) The static structure factor $S(Q)$ at 1223 K for $Al_{72.1}Pd_{20.7}Mn_{7.2}$ obtained by a neutron diffraction experiment [6].

$Q = 6$ nm^{-1} arise from those in the profile of $J_l(Q, \omega)$ in figure 1(b), that is, the substantial broadening accompanied by an increasing weight of high-frequency modes in the distribution. Also, in figure 2(c), it seems that the effective sound velocity $v(Q)$ jumps between $Q = 5.5$ and 6.9 nm^{-1}, that is, the crossover of $v(Q)$ from hydrodynamic to viscoelastic regions occurs at approximately 6 nm^{-1}. Thus, these results strongly suggest that a change occurs in the micro-dynamics peculiar to $Q = 6$ nm^{-1} in the $Al_{72}Pd_{20}Mn_8$ melt near the melting point.

We consider that the change of $v(Q)$ around 6 nm^{-1} could be attributed to the existence of a cluster in the melt. When the wavelength of sound decreases and becomes comparable with the cluster size, $v(Q)$ is expected to be faster if the density of the cluster were larger than the average density and the bonds of the intra-cluster were stronger than those of the inter-cluster. This speculation may be reasonable when the recent experimental studies on the electron density distribution of α-Al(Mn, Re)Si approximant crystals [14, 15] are taken into account. These approximant crystals are known to exhibit quasicrystal-like electrical properties and possess a icosahedrally symmetric cluster. It was reported that covalent bonds are clearly observed in the Al (or Si) icosahedral cluster, or between Al and Mn or Re atoms. In addition, recent diffraction studies on $Al_{13}(Co, Fe)_4$ melts that form approximants on cooling have strongly suggested the existence of dodecahedral clusters of about 0.8 nm diameter [16]. These results encourage us to believe in the existence of such clusters which consist of strongly bonded atoms in the present melt. The cluster size is estimated to be about 1 nm in diameter from the fact that the positive jump of $v(Q)$ and also the broadening of $J_l(Q, \omega)$ occur approximately at 6 nm^{-1}. The cluster size is consistent with that of the dodecahedral clusters in $Al_{13}(Co, Fe)_4$ melts [16]. The faster sound waves may exist around the limited space of clusters so the lifetime of the sound may be short, which is a possible origin for the large broadening of $J_l(Q, \omega)$.

In summary, we have studied the dynamics in the melt of an icosahedral $Al_{72}Pd_{20}Mn_8$ QC near the melting point in the range of momentum transfer below the first maximum position of the static structure factor of the melt. We obtained the dynamical structure factor and the dispersion curve for the first time. The effective sound velocity is abruptly changed and the longitudinal current–current correlation function is substantially broadened at approximately 6 nm^{-1}. These changes are considered to indicate the existence of a cluster of about 1 nm. To confirm the present observation and to obtain detailed information on the cluster, small-angle x-ray scattering measurement would be helpful. We are now pursuing this for the $Al_{72}Pd_{20}Mn_8$ melt.

Acknowledgements

We are grateful to Professor Kaoru Kimura and Professor Yoshihiko Yokoyama for illuminating discussions. The measurements at SPring-8 were performed with the approval of JASRI (Proposal No 2004A 0510-ND3d-np). This work was supported in part by a Grant-in-Aid from the Ministry of Education, Culture, Sports, Science and Technology of Japan and the Light Metal Educational Foundation Incorporated. JTO is grateful for the support of RIKEN Special Postdoctoral Researchers Program.

References

[1] Shechtman D, Blech I, Gratias D and Cahn J W 1984 *Phys. Rev. Lett.* **53** 1951
[2] Stadnik Z M 1999 *Physical Properties of Quasicrystals* (*Springer Series in Solid-State Sciences* vol 126) (Berlin: Springer)
[3] Yokoyama Y, Miura T, Tsai A P, Inoue A and Masumoto T 1992 *Mater. Trans. JIM* **33** 97
[4] Ishikawa R, Ishikawa T, Okada J T, Watanabe Y and Nanao S 2006 *Phil. Mag.* at press
[5] Assael M J, Kakosimos K, Banish R M, Brillo J, Egry I, Brooks R, Quested P N, Mills K C, Nagashima A, Sato Y and Wakeham W A 2006 *J. Phys. Chem. Ref. Data* **35** 285
[6] Simonet V, Hippert F, Klein H, Audier M, Bellissent R, Fischer H and Murani A P 1998 *Phys. Rev.* B **58** 6273
[7] Simonet V, Hippert F, Audier M and Bellissent R 2001 *Phys. Rev.* B **65** 024203
[8] Kelton K F, Lee G W, Gangopadhyay A K, Hyers R W, Rathz T J, Rogers J R, Robinson M B and Robinson D S 2003 *Phys. Rev. Lett.* **90** 195504
[9] Holland-Moritz D, Schenk T, Simonet V and Bellissent R 2006 *Phil. Mag.* **86** 255
[10] Baron A, Tanaka Y, Miwa D, Ishikawa D, Mochizuki T, Takeshita K, Goto S, Matsushita T, Kimura H, Yamamoto F and Ishikawa T 2001 *Nucl. Instrum. Methods* A **467/468** 627
[11] Tamura K, Inui M and Hosokawa S 1999 *Rev. Sci. Instrum.* **70** 144
[12] Scopigno T, Balucani U, Ruocco G and Sette F 2000 *Phys. Rev. Lett.* **85** 4076
[13] Scopigno T, Balucani U, Ruocco G and Sette F 2000 *Phys. Rev.* B **63** 011210
[14] Kirihara K, Nakata T, Takata M, Kubota Y, Nishibori E, Kimura K and Sakata M 2000 *Phys. Rev. Lett.* **85** 3468
[15] Kirihara K, Nagata T, Kimura K, Kato K, Nishibori E, Takata M and Sakata M 2003 *Phys. Rev.* B **68** 14205
[16] Schenk T, Simonet V, Holland-Moritz D, Bellissent R, Hansen T, Convert P and Herlach D M 2004 *Europhys. Lett.* **65** 34